The effect of insulator charging on breakdown and conditioning

The Effect of Insulator Charging on Breakdown and Conditioning

J. M. Wetzer and P. A. A. F. Wouters

High Voltage and EMC Group,
Eindhoven University of Technology, The Netherlands

ABSTRACT

As part of a study on HV design concepts for microwave tubes, a number of different insulator designs have been studied. Analysis of the measured dc current, partial discharge activity and breakdown voltage shows that surface charging of insulators is a key mechanism in the breakdown process and in the conditioning process. Insulator parameters are not only the breakdown voltage, but also the conditioning speed, and the sensitivity to gas exposure or charge leakage. In all these respects insulators with a field enhancement at the anode are superior. Field enhancements at the cathode are less harmful if stepped insulator shapes are chosen. Effective conditioning requires at least a limited number of breakdowns. With sufficient conditioning breakdowns, all insulator geometries tested reached a breakdown field exceeding 12 kV/mm.

1. INTRODUCTION

MODERN satellites are equipped with high-frequency amplifiers for communication purposes or for the operation of radar systems. The most common type of amplifier used is the traveling-wave tube (TWT) amplifier. A TWT consists of an electron gun which produces an electron beam, an interaction area where energy is transferred from the electron beam to the high-frequency signal, and an electron collector which retards and collects the electrons. TWT's operate at voltages of typically 5 kV for continuous wave tubes (communication) up to 25 kV for pulsed tubes (radar). The corresponding average field strength values vary between 10 and 100 kV/cm.

The present generation of spacecraft TWT suffers from occasional tube failure as a result of spurious discharges and HV breakdown. Future designs tend towards smaller dimensions (required because of the higher frequencies used) and higher voltages (for more power). The work presented is part of a study on HV design concepts and guidelines for future microwave tubes, and is supported by the European Space Agency [1].

In this paper the results related to surface charging of insulators will be presented. Some theoretical considerations are discussed, concerning the impact of surface charge on the (cathode) field, and the external current due to charging processes. The experiments reported include measurement of the dc emission-current evolution in time, partial discharge activity, and the breakdown voltage and its evolution in time. Earlier we have reported on the time-resolved measurement of current and optical emission during breakdown (bandwidth 600 MHz), and on the experimental comparison of different conditioning procedures [1–3].

Many researchers have reported on the impact of insulator design on the breakdown voltage [4–7], and on surface charging of insulators [8–11]. In the present work

0018–9367/93/ $3.00

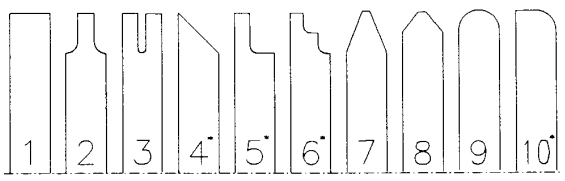

Figure 1.

Insulator geometries used in the present study (asymmetric shapes denoted * are tested both ways). Insulator material Al_2O_3, thickness 5 mm, radius 20 mm. The dash-dot line is the axis of symmetry.

we have studied the charging process for different insulator designs. In particular we will discuss the impact of charging processes on the breakdown voltage and the conditioning process, and the implications of charging processes for the insulator design.

2. EXPERIMENTAL ARRANGEMENTS

THE experimental setup and the diagnostics have been presented in detail elsewhere [1–3], and will be outlined only briefly here. The experiments are performed in a stainless steel vacuum vessel, at a pressure of 10^{-4} to 10^{-5} Pa. Disk-shaped insulator test samples are placed between a pair of OFHC copper electrodes, in a region of homogeneous field. The electrode edge radii are chosen sufficiently large to limit the field. The HV electrode (cathode) is connected to a 60 kV HV supply through a vacuum feedthrough and a damping resistor. The low-voltage electrode (anode) is connected to ground through a measuring impedance (which depends on the type of measurements performed). The electrodes are regularly remachined. The vessel is equipped with (quartz) viewing ports for optical emission measurements. Partial discharge (PD) measurements require a high-frequency circuit for the PD current pulse to flow. For this purpose a 500 pF coupling capacitor is used during PD measurements only.

The test samples are shown in Figure 1. The shapes chosen are representative for insulator geometries found in actual tube designs. All samples are machined out of circular disks of 40 mm diameter and 5 mm thickness, made of Wesgo AL300 alumina, metalized at top and bottom side with MoMn and Ni, and gold plated. The outer surfaces are carefully machined under clean room (dust free) conditions, to a surface roughness below 0.2 μm. The disks are cleaned in flowing ethanol of 70°C, dried and stored in dry nitrogen. With an optical microscope and a scanning electron microscope (SEM) samples are inspected in different stages of production (virgin/metalized/machined disks), as well as before and after experiments.

The diagnostics include dc emission-current measurements (sensitivity 0.05 pA), dc PD measurements (sensitivity 0.2 pC), and series of breakdown voltage measurements, with limited energy. A noncontacting technique is used to remove surface charge and thereby study its effect on the breakdown behavior. This charge removal is performed by admitting nitrogen to a pressure beyond the Paschen minimum, with no voltage applied. The HV source and most diagnostics are controlled and monitored by a personal computer. The sensitivities mentioned are made possible by our well-screened HV laboratory. State of the art EMC measures are taken to ensure reliable and interference-free measurements in the presence of flashovers, PD, switched mode power supplies and other sources of interference.

Before the experiments the samples are conditioned. Earlier, we have compared different conditioning techniques [1–3]. It was found that conditioning becomes more effective if a few breakdowns are permitted. The experiments further showed that the conditioning effect may be lost when the component is exposed to low-pressure nitrogen. When nitrogen was admitted to samples after voltage application, but with the electrodes grounded, discharges were observed as a result of the charges accumulated at the insulator surface. Different conditioning procedures have been tested in which we have combined dc current conditioning (at stepwise increasing voltages) and breakdown conditioning. From this comparison we have adopted the following step-conditioning procedure: the voltage is ramped to breakdown; the voltage is then set at 90% of this first breakdown voltage for 5 min, and is increased by 5% every 5 min until a next breakdown occurs; the voltage is then set at 90% of this second breakdown value, and so on, until a preselected number of breakdowns has occurred (in this case 6). For this procedure, as compared to others, the breakdown voltage shows a fast rise and a small spread.

3. STUDY OF SURFACE CHARGING PROCESSES

3.1 THEORETICAL CONSIDERATIONS

Whereas many secondary processes have been suggested in the literature, primary electron emission caused by electric fields is clearly considered to be the starting point

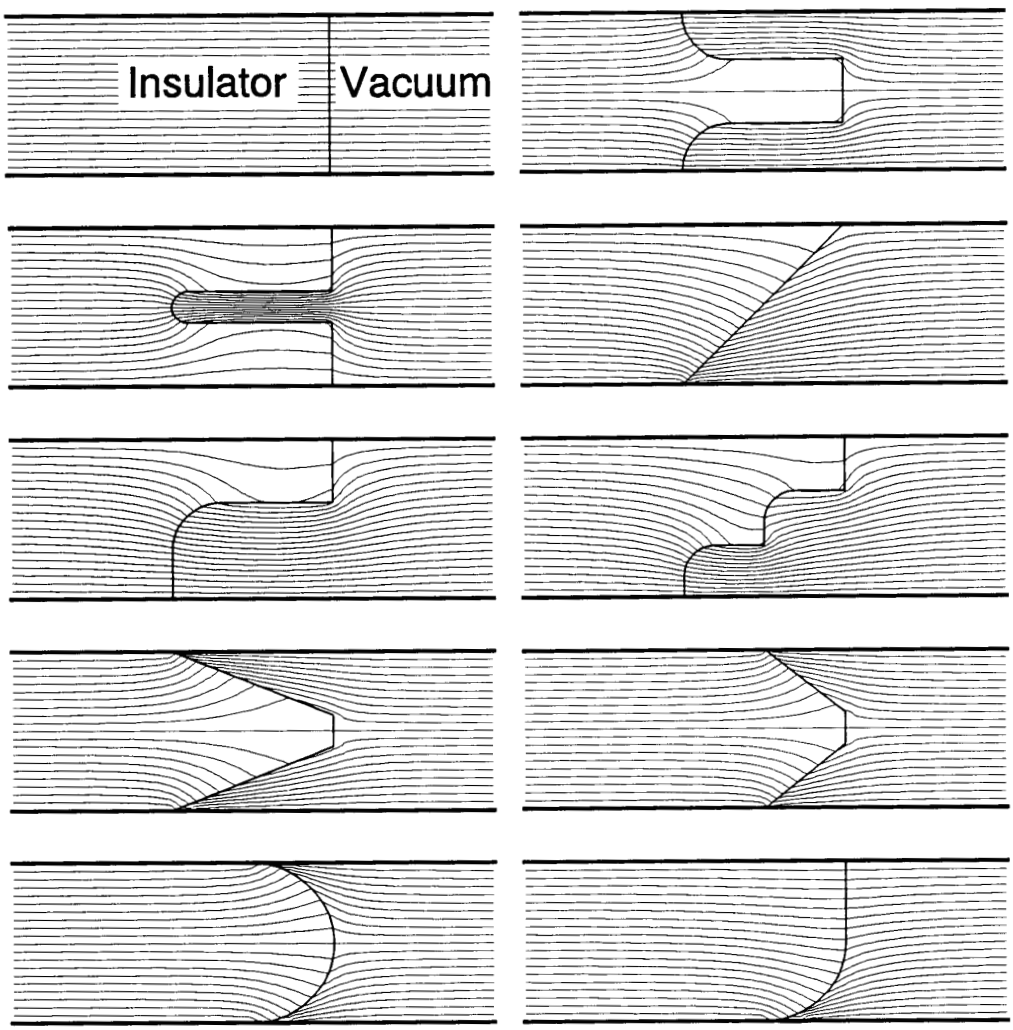

Figure 2.

Equipotential line plots for all geometries of Figure 1, generated with a BEM program. The left side of each plot represents the dielectric, the right side is the vacuum side.

of every breakdown or flashover event [12, 13]. When improving the HV performance of insulators, the first aim should therefore be to reduce or eliminate primary emission from the cathode, usually from the cathode triple junction [14], by reducing the local electric field strength. Field calculations are a helpful tool in the study of design implications. For this work we have used the program ELEKTRO (Integrated Engineering Software Inc, Winnipeg), which is based on the boundary element method (BEM) (see for example [15]). Figure 2 shows plots of equipotential lines, for all insulator geometries shown in Figure 1, with no surface charge present. The macroscopic field plots do not show the microscopic field enhancements which are responsible for electron emission. However, since the local field values are the product of the macroscopic field and a field enhancement factor caused by microscopic protrusions, these enhancements are less harmful in regions with low macroscopic field.

Many researchers have reported on surface charge as a parameter in surface flashover. Surface charge may enhance the cathode field and thereby stimulate breakdown, or it may reduce the cathode field and thereby improve the voltage withstand capability. As an example of a cathode field reduction Figure 3 shows a BEM-plot of equipotential lines for a negatively charged insulator.

The surface charge density may be derived from the measured field in front of the surface, using the correct

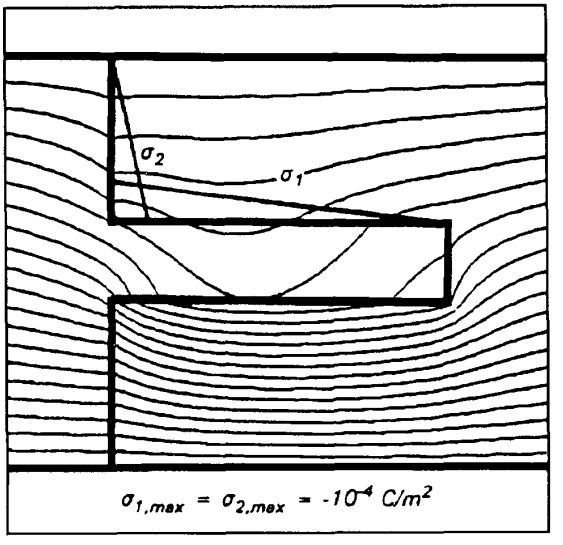

Figure 3.

Equipotential line plot for a negatively charged flat cylindrical insulator (top is cathode). Horizontal and vertical surfaces have a linear charge distribution varying from zero at the edges to a maximum charge density of 100 μC/m^2.

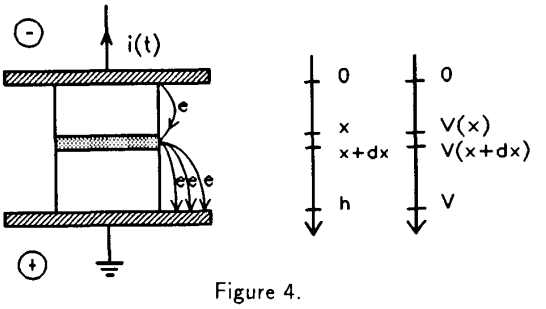

Figure 4.

Simplified model used in the present analysis.

expression for $\kappa = \sigma/E$. For a conducting surface we find $\kappa = \varepsilon_o$, for a dielectric foil $\kappa = 2\varepsilon_o$, and for a dielectric half space $\kappa = \varepsilon_o(\varepsilon_r + 1)$. An expression often quoted in the literature is $E = \sigma/2\varepsilon_o$. By the use of this incorrect relationship, surface charge fields may be overestimated by a factor of $(\varepsilon_r + 1)/2$.

In this work information on charging processes is derived from externally measured quantities: dc current evolution in time, PD activity and breakdown behavior. The relation between charging processes and external current (or charge) is discussed in terms of the simplified model of Figure 4.

For a cylindrical sample of radius R we assume that $N_e(t)$ electrons leave the cathode per second and per unit length of triple junction. Each electron leaving the cathode hits the insulator surface once, thereby releasing γ secondary electrons. We consider the insulator segment between x and $x+dx$. The number electrons that hit this segment per second and per unit length of circumference is $n_e(x,t)dx$. The number of electrons which leave the same segment per second and per unit length of circumference and move towards the anode, is $\gamma n_e(x,t)dx$. The quantities $N_e(t)$ [m^{-1}s^{-1}] and $n_e(t)$ are related as

$$\int_0^h n_e(x,t)dx = N_e(t) \tag{1}$$

For each electron which moves from 0 to x, a charge $eV(x)/V$ flows through the external circuit. An electron moving from from x to d causes an external transport of charge equal to $e[V - V(x)]/V$ [16]. Here V is the voltage difference between the electrodes, and $V(x)$ is the potential at position x. Defining $\lambda(x) = V(x)/V$, and integrating over the whole insulator surface, the external current is obtained

$$\begin{aligned} i(t) &= \int_0^h j(x,t)\,dx \\ &= \int_0^h 2\pi R e n_e(x,t)[\lambda(x) + \gamma\{1 - \lambda(x)\}]\,dx \end{aligned} \tag{2}$$

where $j(x,t)$ is a 1-dimensional current density (of dimension Cm^{-1}s^{-1}). We further introduce a 1-dimensional charging current density $_s(x,t)$ as

$$j_s(x,t) = -(1-\gamma)2\pi R e n_e(x,t) \tag{3}$$

Over a time T the charging current causes an accumulation of surface charge with density $\sigma(x)$ [Cm^{-2}]

$$\sigma(x) = \frac{1}{2\pi R}\int_0^T j_s(x,t)\,dt \tag{4}$$

Eliminating γ we can relate the current densities $j(x,t)$ and $j_s(x,t)$, and reformulate the expression for the external current

$$j(x,t) = 2\pi R e n_e(x,t) + j_s(x,t)[1 - \lambda(x)] \tag{5}$$

$$i(t) = 2\pi R e N_e(t) + \int_0^h j_s(x,t)[1 - \lambda(x)]\,dx \tag{6}$$

The amount of charge which flows through the external circuit in a time T is given by

$$q_{app} = 2\pi Re \int_0^T N_e(t)\,dt + 2\pi R \int_0^h \sigma(x)[1-\lambda(x)]\,dx \quad (7)$$

As in the evaluation of PD measurements we use the term 'apparent charge' here because the measured charge gives only an indirect representation of the actual charges that are moving in the gap or collected by the surface (see also [16]). In both Equations (6) and (7) the first term corresponds to electron emission at the cathode, and the second term corresponds to surface charging. The outcome is independent on γ. For a (crude) first order approximation we assume that: the emission current is constant; the charge density is uniform: $\sigma(x) = \text{constant}$; and that the field is uniform: $\lambda = x/h$. We then find

$$q_{surf,app} = \tfrac{1}{2} q_{surf} \quad (8)$$

in other words, half of the charge accumulated at the insulator surface is reflected in the measured charge. In general, the evaluation of surface charge from measured current or charge is more complicated.

Charging processes take place on time scales varying from $\sim 4\ \mu s$ to ~ 3 min. The diagnostics used are operational on different time scales and should therefore be regarded as complementary.

3.2 dc CURRENT ANALYSIS

The dc current measurements are carried out at three equidistant voltage levels, following an 'up and down' method as shown in Figure 5. The highest voltage level is chosen $\sim 20\%$ below the breakdown voltage (as determined during the conditioning procedure). The voltage is maintained at each level for 15 min, or longer if necessary. Upon each voltage increase the current increases stepwise and then decays to an end value.

Figure 6 shows a typical example of the current measured upon a voltage step. During the first ~ 30 s the current is dominated by a displacement current caused by the voltage supply: after a change of the voltage it takes some time to settle down to a stable voltage level (note that a change of 1 V/s causes a displacement current of ~ 25 pA). This spurious current has an RC behavior, and is incorporated in a response function F_{resp}. This function also involves the response of the measuring setup, including filter, amplifier and electrometer, and is determined prior to the experiments [1]. The measured

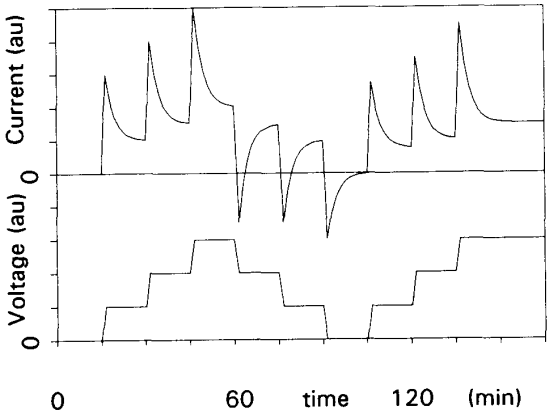

Figure 5.

Voltage (lower trace) and current (upper trace) *vs.* time (a.u.) for the dc current measurement.

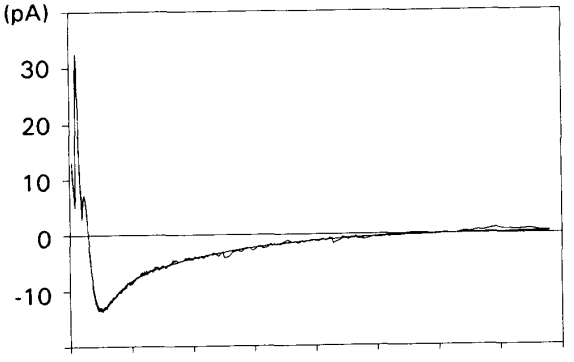

Figure 6.

An example of measured dc current (pA) *vs.* time (s), and corresponding fit, at a voltage step from 4.1 to 10.4 kV. The early part of the current is dominated by a displacement current. A jump in the current corresponds to an increase in the sensitivity with a factor of 10. Both effects are corrected in the fit (see Equation (5)).

current $i_{exp}(t)$ is then fitted using the response function and a function describing the 'real' prebreakdown current, which corresponds to $i(t)$ in Equation (6). The latter consists of a constant (the final field-emission current, i_e) and two (sometimes three) exponentials (see Equation (9))

$$\begin{aligned} i_{exp}(t) &= F_{resp}[i(t)] \\ &= F_{resp}[i_e + i_1 e^{-t/\tau_1} + i_e e^{-t/\tau_2}] \end{aligned} \quad (9)$$

If the voltage is not close to the breakdown value, this function gives an excellent fit (see Figure 6). The fitting functions are then used to derive the end value of the current, the time constants of the current decay, and the

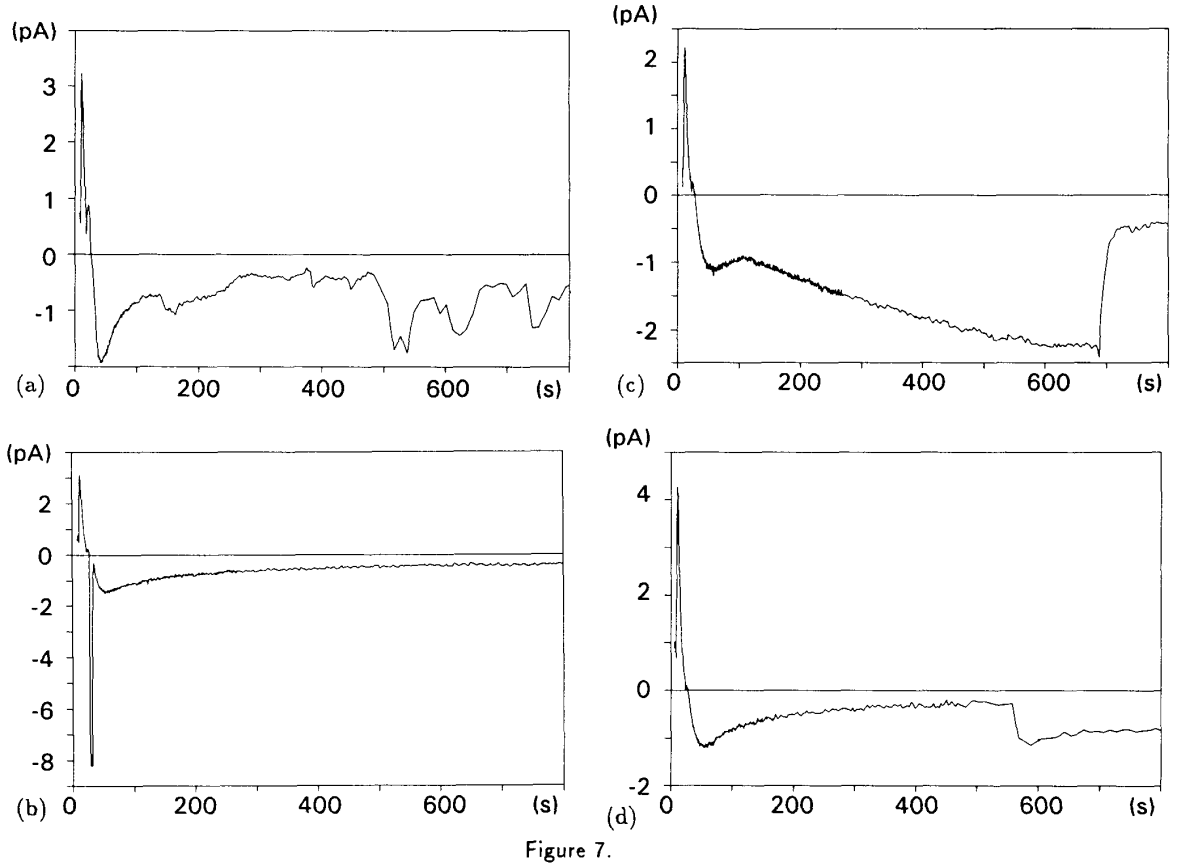

Figure 7.

Examples of nonexponential current decay upon a stepwise voltage change, at voltages close to breakdown. Currents in pA, time in s. (a) unstable current at voltage near breakdown, (b) filtered response to PD, (c) extinction of cathode emission site ($t = 690$ s), (d) initiation of cathode emission site ($t = 560$ s).

amount of charge that has passed. For voltages close to the breakdown voltage, the current is not well described by the exponential decay [1, 2]. In Figure 7 some examples are given corresponding to (a) an unstable current, (b) a PD, (c) extinction and (d) initiation of an emission site.

Two samples of each shape were tested. For the end value of the current, the differences between identical samples were in the order of the measured current. For most samples the end current at 20 kV is ~ 0.2 pA, and increases strongly when the voltage approaches breakdown. The end current at a specified voltage is not a solid basis for comparison, the 'near breakdown' value might be more meaningful.

The time constants for the exponentials are 16 and 150 s, and do not depend on the sample shape. If we define one overall time constant, the value would be ~ 110 s for all samples.

The total amount of charge corresponding to the step-response transient is derived by integration of the measured current, after subtraction of the end current (compare Equation 7)

$$q_{transient} = \int_{t=0}^{\infty} [i(t) - i_e]\, dt \qquad (10)$$

Since equidistant voltage steps appeared to give approximately the same amount of charge, a charge per voltage step is defined. The first and second voltage rise result in approximately the same amount of charge, as do a voltage rise and a voltage drop. The results are shown in Figure 8, and show a clear and reproducible difference between shapes. For samples 4a and 8 the spread is large as a result of the low initial breakdown voltage, and the fact that, close to breakdown, the dc current is unstable.

The observations that equidistant voltage steps give approximately the same amount of charge, and a volt-

age rise and a voltage drop give approximately the same amount of charge, indicate that the insulator surfaces are charged and discharged upon stepwise voltage changes. An explanation in terms of polarization relaxation (a bulk mechanism) is contradicted by the clear and reproducible difference between sample shapes. Application of the simplified model (Section 3.1) yields surface charge densities of $\sim 0.15\ \mu C/m^2$. Most literature values are in the order of 0.5 to 1 $\mu C/m^2$. The difference may be due to the fact that the samples have been conditioned prior to the dc current measurements, or due to incorrect evaluation of measured fields (Section 3.1). On the other hand, we may conclude that a substantial part of the surface charge is accumulated on a time scale of ~ 2 min.

3.3 PARTIAL DISCHARGE ANALYSIS

PD has been measured during and following ramp changes of the applied voltage, as shown in Figure 9. The ramp speed was low in order to prevent that its displacement current would be counted as a PD. An example of a PD measurement during a voltage rise from 10 to 20 kV is shown in Figure 10. The PHA plot (pulse height analysis) shows the number of counts *vs.* discharge amplitude, and the MCS plot (multi-channel scaling) shows all counts exceeding a preset threshold (0.3 pC in the present work) *vs.* time. The PHA plot gives the usual pattern of decreasing counts with increasing amplitude. The MCS plot indicates that most discharges occur during the voltage rise (the first 10 s). This observation again indicates that the insulator surfaces are charged and discharged upon stepwise voltage changes. Summation of all measured charges gives the total charge passed upon a given voltage step. This charge is (by chance probably) of the same order of magnitude as that derived from the dc current measurements ($\sim$ 25 pC/kV). The reproducibility is poor, and no clear correlation with sample shape was found.

3.4 BREAKDOWN VOLTAGE ANALYSIS

The breakdown voltage evolution is measured by repeatedly ramping the voltage to breakdown. Upon each breakdown the voltage is reset to zero and, after a delay of 3 s, again ramped to breakdown. This is repeated until the breakdown voltage exceeds the 60 kV maximum supply voltage. Then the surface charge is removed and the procedure is repeated. Charge removal is performed in a noncontacting way, by admitting nitrogen to a pressure beyond the Paschen minimum, with no voltage applied.

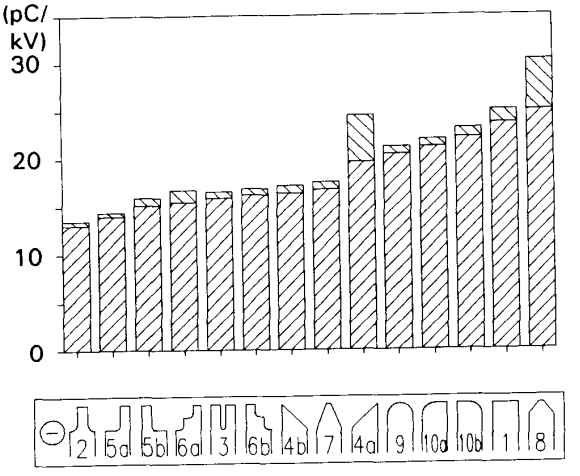

Figure 8.

The charge per voltage step (pC/kV) derived from dc current measurements. For each sample the average value and the spread is given. The values are averaged over both samples and over all voltage steps in one dc measurement (see Figure 5).

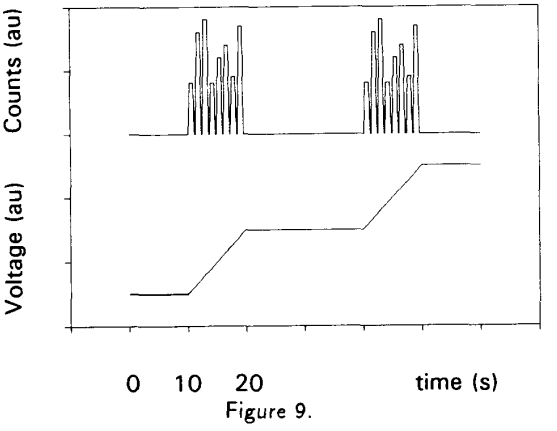

Figure 9.

Voltage (lower trace) and PD activity (upper trace) *vs.* time (a.u.) for the PD experiments.

During nitrogen admission, optical emission and PD activity indicate that the surface is indeed being discharged. After charge removal the vessel is pumped down again. The breakdown energy is limited to the energy capacitively stored in the test geometry (maximum 45 mJ at 60 kV). An example of a breakdown voltage measurement is given in Figure 11.

The breakdown voltage increases to $\sim 4\times$ its initial value, and falls back upon exposure to nitrogen. This proves that surface charge may dramatically affect the breakdown voltage. In the series of breakdowns after ex-

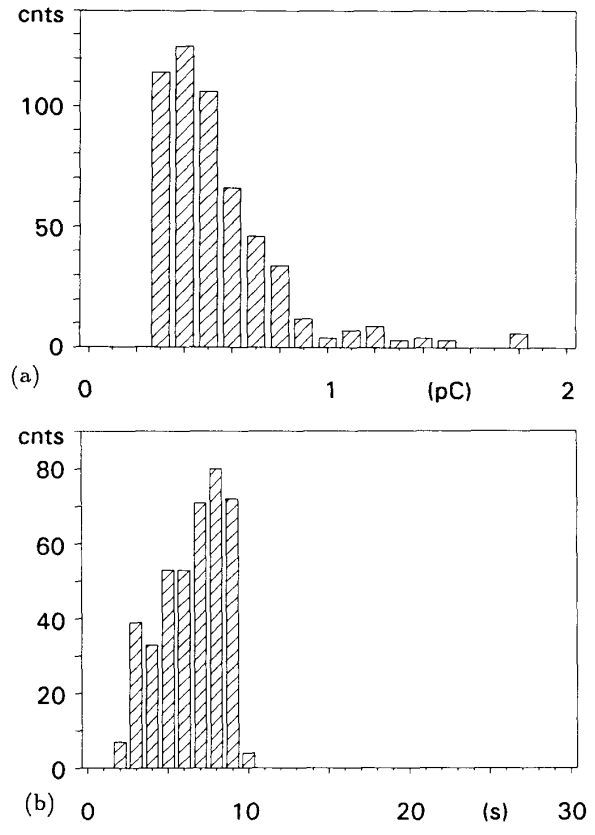

Figure 10.

PD measurement during a ramped voltage increase from 10 to 20 kV at a rate of 1 kV/s. Duration 1 min, sample 1. (a) PHA plot: counts *vs.* charge, (b) MCS plot: counts exceeding threshold *vs.* time.

posure, the insulator is conditioned much faster than in the first one. This clearly shows that also an irreversible conditioning process has taken place during the first series of breakdowns.

Important insulator parameters are the breakdown voltage (before and after conditioning), the conditioning speed, and the dependence on surface charge. Figure 12 shows the minimum breakdown voltage (before conditioning or nitrogen exposure) for different insulator shapes.

All insulators tested reached a breakdown voltage of 60 kV. Figure 13 shows the first breakdown voltage after nitrogen exposure. Figure 14 gives the number of breakdowns needed to reach a breakdown voltage level of 50 kV, before and after the surface charge is removed. A summary of the results of the breakdown voltage experiments is presented in Table 1.

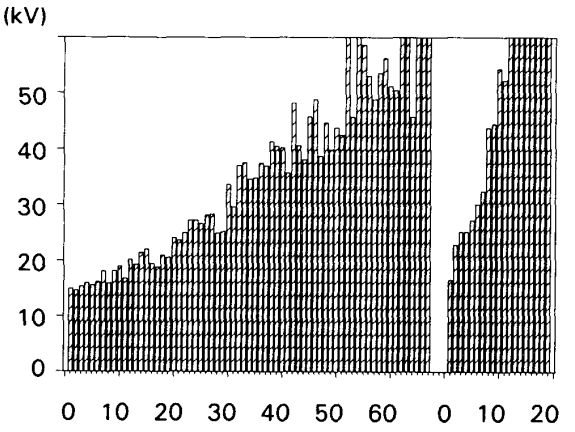

Figure 11.

Measured breakdown voltage (kV) *vs.* breakdown number for insulator 4(a) (geometry 4 from Figure 1 with field enhancement at cathode side). The left series (1–67) is recorded before, the right series (1–19) after exposure to low pressure nitrogen.

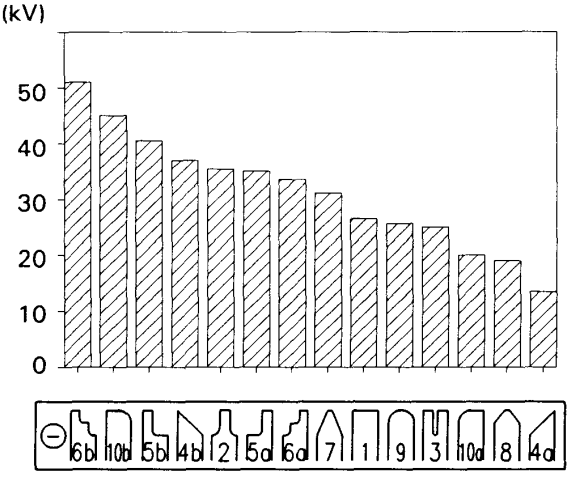

Figure 12.

Minimum (usually first) breakdown voltage observed (kV), in ranking order. Two samples of each geometry were tested. Each bar presents the average value.

Geometries for which the field at anode, with no surface charge present, is enhanced (4(b), 5(b), 6(b), 10(b)) show the highest breakdown voltage (compare also the field plots in Figure 2). Note that at a given voltage the integral $\int E\,dl$ is constant and a field enhancement at the anode causes a field reduction at the cathode. Further, the conditioning speed is high and the breakdown voltage hardly changes by nitrogen exposure: these samples hardly collect surface charge.

Table 1.

Summary of the results of the breakdown experiments. Top side of sample geometries is cathode. The averaged breakdown field is defined as the breakdown voltage over electrode distance. All values are averaged over two samples.

Sample	Averaged breakdown field (kV/mm) MINIMUM	Averaged breakdown field (kV/mm) MAXIMUM	Averaged breakdown field (kV/mm) CHARGE REMOVED	Number of breakdowns to reach 10 kV/mm	Breakdown energy (mJ)
6b	10.2	>12	11.3	0	33-45
10b	9.0	>12	>12.0	1	25-45
5b	8.1	>12	10.7	8	21-45
4b	7.4	>12	>12.0	5	17-45
2	7.1	>12	9.3	36	16-45
5a	7.0	>12	11.8	24	15-45
6a	6.7	>12	11.3	45	14-45
7	6.2	>12	7.0	40	12-45
1	5.3	>12	>12.0	78	9-45
9	5.1	>12	9.3	61	8-45
3	5.0	>12	9.0	188	8-45
10a	4.0	>12	5.4	25	5-45
8	3.8	>12	5.2	109	5-45
4a	2.7	>12	3.5	71	2-45

For geometries with a field enhancement at the cathode the breakdown voltage and the conditioning speed is lower, and a difference is observed between stepped (2, 5(a), 6(a)) and non-stepped shapes (4(a), 7, 8, 9, 10(a)). The stepped shapes have a higher breakdown voltage, and do not rely heavily on surface charge in order to attain a high breakdown voltage.

For non-stepped shapes a 45° angle (4(a), 8) causes a lower breakdown voltage than geometries with a smaller angle (7); as with stepped shapes, a small angle improves the effectiveness of charge collection, thereby reducing the cathode triple junction field.

4. DISCUSSION AND CONCLUSIONS

THE two key mechanisms for surface flashover of insulators are primary electron emission and surface charging. Primary electron emission from negative electrodes (cathodes) can be reduced most effectively by concentration of the electric field at the positive electrode (anode). Surface charging should either be avoided or used to advantage: properly shaped insulators can trap charges during conditioning such as to reduce the cathode field.

The work presented clearly proves the presence of surface charge and its effect on the breakdown voltage and on the conditioning process. The dc current measurements and the PD measurements indicate that the insulator surfaces are charged and discharged upon stepwise voltage changes. Evidence for the presence of surface charging is found in the breakdown voltage experiments: if, after a series of breakdowns, a sample is exposed to nitrogen *with no voltage applied and with both electrodes grounded*, a discharge is observed both optically and electrically. The only possible source producing the electric field for such a discharge is the charge accumulated at the insulator. The difference in breakdown behavior before and after

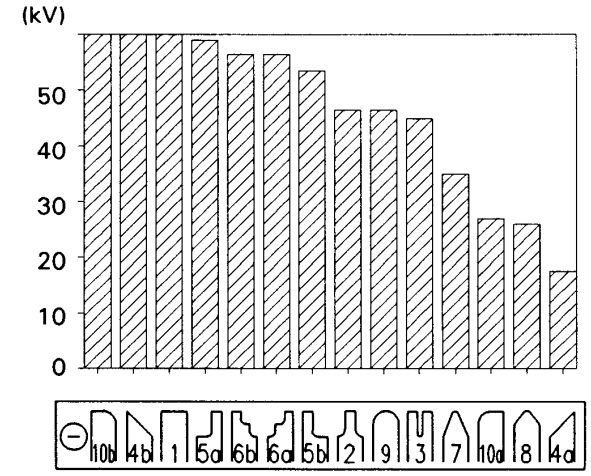

Figure 13.

First breakdown voltage after N_2 exposure (kV), in ranking order. Two samples of each geometry were tested. Each bar presents the average value. The breakdown voltage before N_2 exposure equals the maximum supply voltage of 60 kV.

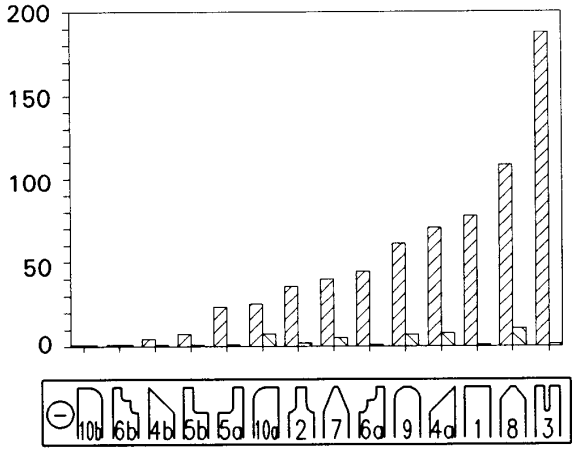

Figure 14.

Number of breakdowns needed to establish a breakdown voltage of 50 kV, before (left bar) and after (right bar) N_2 exposure. The samples are ranked according to the number of breakdowns required before exposure. Two samples of each geometry were tested. Each bar presents the average value.

nitrogen exposure can then be attributed to the effect of surface charge.

Parameters describing the quality of insulators in vacuum are the breakdown voltage values (before and after conditioning), the conditioning speed, and the dependence on surface charge. Given sufficient conditioning breakdowns, all insulating geometries tested attain a high breakdown voltage. Insulators that rely on surface charge in order to have a high breakdown voltage loose their conditioning effect when they are exposed to whatever gas, or when they are left without voltage applied for too long a time (leakage). For the samples used in this study, the breakdown voltage was not affected when the voltage was switched off for a period of about 65 h.

The findings of this work have implications for the design of vacuum insulators, and the appropriate conditioning process. If, in the conditioning process, one applies a sufficiently large number of breakdowns with limited energy, all geometries will reach a high breakdown voltage. If no breakdown conditioning is applied, the minimum or first breakdown voltage is decisive. For practice a limited number of breakdowns is preferable, and a geometry with a high conditioning speed should be chosen. Also in case of repetitive exposure to gases, or when the voltage is frequently switched off for long periods of time, a design with a high conditioning speed should be chosen. In terms of breakdown voltage, sensitivity to exposure or charge leakage, and conditioning speed, insulator geometries with field enhancements at the anode are superior. If cathode field enhancements are unavoidable, stepped shapes are recommended.

Breakdown conditioning, and in particular step-conditioning, may improve drastically the voltage holdoff performance, and reduce the effects of uncontrolled, often microscopic, parameters. Future work should reveal what is the optimum breakdown energy for conditioning if breakdowns are permitted.

The results presented are obtained for alumina insulators. For other insulator materials the same processes will occur but the impact of charging on the breakdown and conditioning process may be different, depending on the secondary emission coefficient and the surface conductivity. The conclusions with respect to optimization of the insulator shape however remain valid since the optimum geometries are those which either do not collect surface charge or can only collect negative surface charge because of geometrical reasons.

ACKNOWLEDGMENT

This study is performed under ESTEC contract no. 7186/87/NL/JG (SC). The contributions of P. C. T. van der Laan, A. J. M. Pemen and M. G. Danikas, and the technical assistance of A. J. Aldenhoven and P. F. M. Gulickx is gratefully acknowledged. The authors want to thank S. J. Feltham for the technical coordination of the contract and for his stimulating interest in the work.

REFERENCES

[1] J. M. Wetzer, P. A. A. F. Wouters, A. J. M. Pemen, M. G. Danikas, P. C. T. van der Laan and A. J. Aldenhoven, "Final Report of the Study on HV-design Aspects of Microwave Tubes", ESA contract no. 7186/87/NL/JG (SC), 1991.

[2] J. M. Wetzer, P. A. A. F. Wouters, P. C. T. van der Laan and A. J. M. Pemen, "Design Aspects of HV Insulators in Vacuum", Proceedings 1991 ESA Workshop on Space TWTA's, Noordwijk, paper 6.1, 1991.

[3] J. M. Wetzer and P. A. A. F. Wouters, "The Design of HV Insulators for Spacecraft Traveling Wave Tubes", 1992 Symposium on Electrical Insulation, Baltimore, June 7–10, pp. 31–35, 1992.

[4] J. P. Shannon, S. B. Philp and J. G. Trump, "Insulation of HV Across Solid Insulators in Vacuum", J. Vac. Sci. Tech., 2, 1965, pp. 234–239.

[5] A. V. Pillai and R. Hackam, "Surface Flashover of Conical Insulators in Vacuum", J. Appl. Phys., Vol. 56, pp. 1374–1381, 1984.

[6] N. C. Jaitly and T. S. Sudarshan, "Novel Insulators Designs for Superior dc Hold-off in Bridged Vacuum Gaps", IEEE Trans. EI, Vol. 22, pp. 801–810, 1987.

[7] O. Yamamoto, T. Hara, T. Nakae and M. Hayashi, "Effects of Spark Conditioning, Insulator Angle and Length on Surface Flashover in Vacuum", IEEE Trans. EI, Vol. 24, pp. 991–994, 1989.

[8] C. H. De Tourreil and K. D. Srivastava, "Mechanism of Surface Charging of HV Insulators in Vacuum", IEEE Trans. EI, Vol. 8, pp. 17–21, 1973.

[9] T. S. Sudarshan, J. D. Cross and K. D. Srivastava, "Prebreakdown Processess Associated with Surface Flashover of Solid Insulators in Vacuum", IEEE Trans. EI, Vol. 12, pp. 200–208, 1977.

[10] P. A. Arnold, J. E. Thompson, T. S. Sudarshan and R. A. Dougal", 45 Degree Insulator Surface Flashover; A Review and New Results", IEEE Trans. EI, Vol. 23, pp. 17–25, 1988.

[11] N. C. Jaitly and T. S. Sudarshan, "In-situ Insulator Surface Charge Measurements in Dielectric Bridged Vacuum Gaps Using an Electrostatic Probe", IEEE Trans. EI, Vol. 23, pp. 261–273, 1988.

[12] R. V. Latham, *HV-Vacuum Insulation*, Academic Press, 1981.

[13] H. C. Miller, "Surface Flashover of Insulators", IEEE Transactions EI, Vol. 24, pp. 765–786, 1989.

[14] J. M. Wetzer, M. G. Danikas and P. C. T. van der Laan, "Analysis and Improvement of HV Components for Spacecraft Traveling-wave Tubes", IEEE Transactions EI, Vol. 25, pp. 1117–1124, 1990.

[15] C. A. Brebbia and S. Walker, *Boundary Element Techniques in Engineering*, Newnes-Butherworths, London-Boston, 1980.

[16] J. M. Wetzer and P. C. T. van der Laan, "Prebreakdown Currents, Basic Interpretation and Time-resolved Measurements", IEEE Transactions EI, Vol. 24, pp. 297–308, 1989.

This paper is based on a presentation given at the 15th International Symposium on Discharges and Electrical Insulation in Vacuum, Darmstadt, Germany, 6–10 September 1992.

Manuscript was received on 15 May 1993, in revised form 28 May 1993.